SIMULATION ANALYSIS OF FATIGUE STRENGTH IN STEEL HIGHWAY BRIDGES

Adam WYSOKOWSKI
University of Zielona Góra, prof. Z. Szafrana St. 2,
65-516 Zielona Góra, Poland

In this paper, the determination in a theoretical way – by the simulation analysis - of the stress spectra and strength, as well the service life parameters for the structural elements of road bridges is presented. The analytically obtained results have been verified by the results from field tests of selected elements of steel road bridges under the service load. For the simulation calculations, a linear load model of road bridges (presented in the paper) has been applied, derived from author's measurements on structures and concerning traffic on the Polish urban and country roads and bridges. The presented studies and theoretical analyses have proved that the fatigue hazard exists also in road bridges and they have indicated what types of bridges, which bridge elements in what static schemes, which spans and under what service loads, are endangered by the fatigue hazard.

1. INTRODUCTION

Because steel highway bridges "work" in very adverse weather conditions and are subjected to changing loads of different magnitude and duration, a relatively large number of them needs renovation and rebuilding and many of them are near the end of their life.

Currently in Poland about 35% road bridges, of the total 35 thousand, urgently need to be replaced. In these conditions any structural failure poses a hazard to the bridge if no remedial measures are taken. The problem becomes increasingly pressing as each year the number of old steel highway bridges increases. Therefore decisions should be made whether these bridges can remain

in service after their design life is over or, depending on their importance, they should be reinforced or replaced.

All those factors and the rapid development of the road transport in Central Europe create an urgent need to determine, comprehensively, the effect of moving loads on the fatigue strength of the structural elements of highway bridges.

Since the field investigations of bridge structures are time-consuming and laborious, it would be extremely difficult to carry out a large number of them to obtain the results representative for various kinds of bridge elements, having different static schemes and cross-sections, located on the routes of roads having different volumes and structure of traffic. Furthermore, the results following from field investigations are influenced by a number of other factors.

Therefore, it seems sensible to apply simulation methods in conjunction with some experience gained from the investigations of actual bridge structures for a wider analysis of the highway bridge fatigue problem.

2. SIMULATION METHOD OF DETERMINING THE STRESS SPECTRA

Simulation is usually defined as "the reproduction of the properties of an actual object, phenomenon or process by means of its model". With advances in computer technology the use of simulation methods has become more universal.

The investigation of a model instead of the actual process is simpler, less laborious and cheaper and it can be conducted repeatedly in a short time.

In the author's opinion, computer simulation in which a deterministic sequence of forces represents the axle loads of vehicles seems to be the most sensible solution. The vehicles move independently of one another within a given traffic lane, and they are spaced apart by at least the length of the influence-line branch for the considered element (for one traffic lane). A similar approach to this problem was adopted in (Baus and Bruls 1981).

If the problem of the service durability problem is to be handled comprehensively, all possible parameters should be taken into account, particularly in the case of highway bridges with a relatively high traffic volume or a large number of traffic lanes. Then the likelihood of the simultaneous passage of several vehicles over the bridge should be taken into consideration. Thus it seems logical to treat the movement of vehicles within a bridge as a random process.

A general flow chart illustrating the simulation method of determining the stress or the reaction range spectra for bridge structural elements is shown in fig. 1.
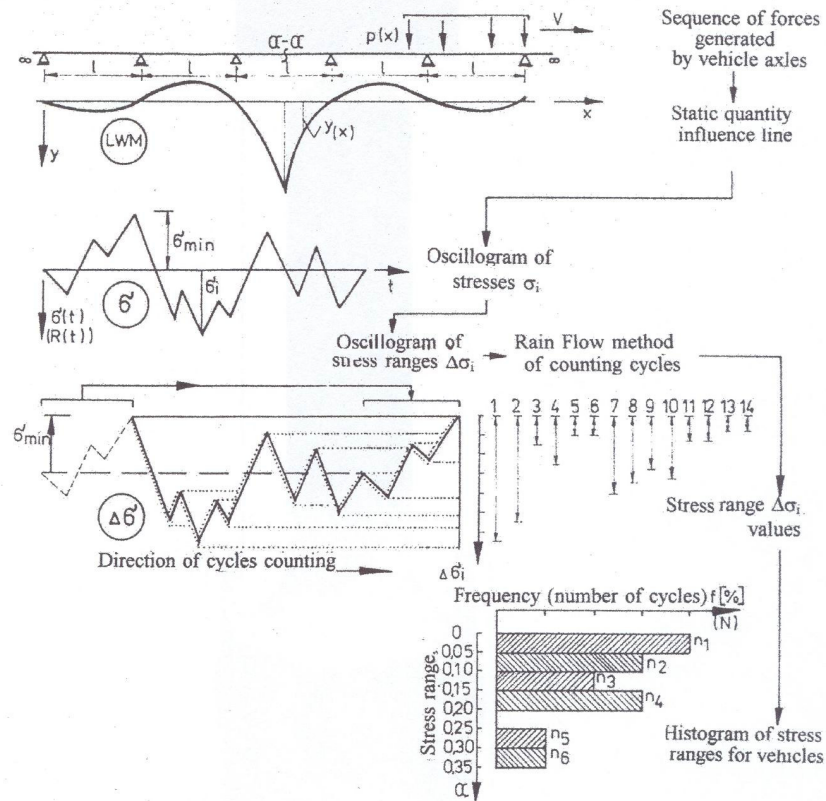
Fig. 1. Procedure for determining the stress ranges or reactions by computer simulation

The values of bending moments (reactions) generated by the sequences of forces "moving" over an influence line can be calculated using the following general formula

$$M(R) = q_k \int_o^l p(x) \cdot y(x) dx \qquad (2.1)$$

where the notations are: q_k – transverse load-distribution coefficient for lane k, $p(x)$ – force values along the length of an influence line, $y(x)$ – ordinates of the influence line of a static quantity (moment or a reaction) for a considered cross-section.

The particular values in the static magnitude oscillograms are calculated for a case when any of the forces, "moving" over the influence line, is situated over its characteristic point, i.e. a zero, maximum or minimum value, as well as over the inflexion point.

An expression for the next value $\Delta\sigma_i$ in the stress oscillogram can be written as follows

$$\Delta\sigma_i = a \cdot \Delta M_i \cdot \varphi_{\Delta actual}, \tag{2.2}$$

with the notations: a – static strength constant, $\varphi_{\Delta actual}$ – dynamic actual-load stress-range coefficient.

Similarly, the stress range generated by standard load $\Delta\sigma_n$ is

$$\Delta\sigma_n = a \cdot \Delta M_n \cdot \varphi_{\Delta s\tan d.} \tag{2.3}$$

where $\varphi_{\Delta stand.}$ is the standard-load stress range dynamic coefficient.

Substituting the expressions (2.2) and (2.3), the relative stress value will be

$$\alpha_i = \frac{\Delta\sigma_i}{\Delta\sigma_n} = \frac{\Delta M_i \cdot \varphi_{\Delta actual}}{\Delta M_n \cdot \varphi_{\Delta s\tan d}}, \tag{2.4}$$

For the analysis of a single bridge structure one can use the expression (2.4), substituting the actual test or experimental values of the dynamic coefficient $\varphi_{\Delta actual,}$ and the appropriately assumed (depending on a static scheme) values of the standard-load stress range dynamic coefficient $\varphi_{\Delta stand}$.

It would be extremely difficult to adopt this approach in the case of complex analysis of different types of bridge structures done on EMC. The reason is that the actual dynamic coefficient $\varphi_{\Delta actual}$ assumes wide-ranging values depending on the kind of bridge structure, the kind and condition of its surface, the way in which vehicles pass over the bridge and the type of the vehicles.

Most often $\varphi_{\Delta actual} \leq \varphi_{\Delta stand}$. Therefore it is advisable to assume for further considerations that $\varphi_{\Delta actual} = \varphi_{\Delta stand}$ which will standardize the calculations and make possible a final comparative analysis of the service strength and the durability for different types of bridge structures. Thus, the calculations done under this assumption are on the safe side.

Taking this into account, the relative stress-range values can be described by the following relation

$$\alpha_i = \frac{\Delta M_i}{\Delta M_n}, \tag{2.5}$$

Another important aspect of the assessment of the service strength of steel bridges, in cases of complex no stationary stress spectra, is the counting of stress-cycle ranges. This problem appears when the obtained stress oscillograms are converted into the stress-range histograms (fig. 1).

There are many methods of counting the stress cycles, e.g. Level Crossing Count, Positive Peak or Range Pairs, which are described in detail in (Baus and Bruls 1981). Neither of these methods takes into account the order in which the cycles occur in a spectrum.

The most universal method of cycle counting is the Rain Flow method described in (Hirt 1977) and (Stier et al. 1982). The advantage which it has over the other methods is that it can be applied directly, i.e. it is not necessary first to reject the short stress cycles. The method is recommended by many international organizations such as ISO (International Organization for Standardization) (Hirt 1983), IIW (International Institute of Welding) (IIW 1981), Eurocode (European Code for Steel Construction) and ECCS (European Convention for Constructional Steelwork) (Carpena 1982). A modification of the Rain Flow method is the Reservoir method recommended for the calculation of road and railway bridges by the British standard (B.S. 1980).

Nevertheless, the Rain Flow method has significant limitations when applied to wider analyses, since it enables only the counting of stress cycles for spectra bearing the same sign, i.e. basically it can be applied only to simple-supported elements (Hirt 1983).

In this paper the author has solved this problem by introducing a useful innovation enabling the counting of cycles for elements with continuous static schemes (changing stress signs), which consists in the prior transformation of the stress spectrum. The author used this modified Rain Flow method to determine the service strength by simulation. The procedure in the case of variable stress signs is shown in fig. 1. First, the stress-oscillogram values σ_{min} are sought. Then all the stress values to the "left" of the minimum value should be moved to the end of the stress oscillogram. Next, the absolute value of the minimum stress σ_{min} should be added to all the stress values. The further steps are similar as in the conventional Rain Flow method, bearing in mind that a full stress-range cycle is made up of two single half-cycles.

The direction in which cycles are counted is indicated by an arrow in fig. 1. Then a histogram of the stress ranges is compiled from the obtained individual stress-range values. In this way, the stress-range spectrum for a single type of vehicle is obtained. The same procedure is applied to other vehicle types. The final result is a comprehensive service-stress-range spectrum for a considered cross-section of a structural element, assembled from the individual-vehicle spectra, which takes into account transverse-load-distribution coefficients for the particular traffic lanes, number-of-vehicles-per-traffic-lane distribution func-

tions and the random model of vehicle traffic on the bridge described in chapter 3. The model takes account of, among other things, the effect of the simultaneous passage of vehicles over the bridge on the obtained static magnitudes and the number of cycles. The service strength and durability parameters were calculated using the formulas and relations compiled below.

For the simulation analysis of the stress spectra and the assessment of service strength and durability of structural elements, the author has developed a software program named "TE-MD" (Service Durability of Road Bridges – in Polish).

Because of the complexity of the problem, three programs in all have been developed. They form a uniform system having the following functions:
1. PROGRAM LW   – for entering influence lines,
2. PROGRAM MOMN – for entering standard moments,
3. PROGRAM TE-MD – determination of sets of stress oscillograms,
                                    – counting of stress-range cycles,
                                    – determination of stress-range histograms and calculation of service strength and durability parameters,
                                    – printout of results.

If the stress spectrum is nonstationary (fig. 2) and all its ranges $\Delta\sigma_i$ cause partial damage, it can be replaced (on the basis of, among others, Miner's hypothesis) by a stationary spectrum with the equivalent stress range $\Delta\sigma_e$ and the actual number of cycles

$$N_r = \sum_{i=1}^{p} n_i \, , \tag{2.6}$$

which occurred in the spectrum [5], and the equivalent stress range $\Delta\sigma_e$

$$\Delta\sigma_e = \left[\frac{\sum_{i=1}^{p} n_i (\Delta\sigma_i)^m}{\sum_{i=1}^{p} n_i} \right]^{\frac{1}{m}} , \tag{2.7}$$

or it can be replaced by a stationary spectrum with on equivalent number of cycles $N_{\Delta n}$ and standard-load stress range $\Delta\sigma_n$

$$N_{\Delta n} = \sum_{i=1}^{p} n_i \left(\frac{\Delta\sigma_i}{\Delta\sigma_n} \right)^m , \tag{2.8}$$

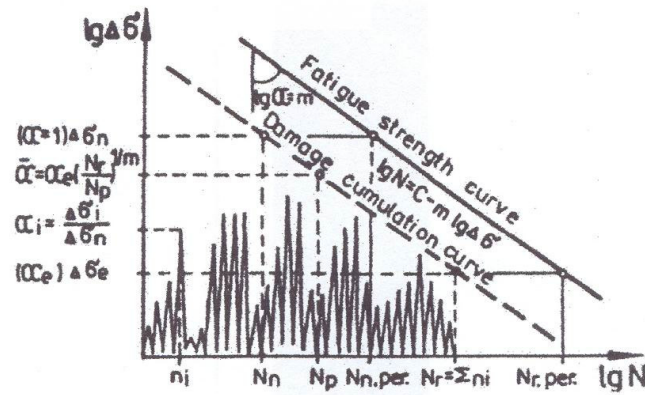where p is the number of stress-range levels in the considered no stationary spectrum.

Fig. 2.   The relationships between stress spectra parameters

In the simulation stress analysis, it is more advantageous to use the relative stress-range level α_i referred to the standard-load stress range $\Delta\sigma_n$ (2.4) and the relative frequency f_i of the number of cycles n_i with level α_i, referred to the total number of cycles in the spectrum

$$f_i = \frac{n_i}{\displaystyle\sum_{i=1}^{p} n_i},$$

(2.9)

If the relations (2.4) and (2.9) are used, the formulas (2.7) and (2.8) become the following forms:

$$\Delta\sigma_e = \Delta\sigma_n \left(\sum_{i=1}^{p} f_i \alpha_i^m \right)^{\frac{1}{m}}$$

(2.10)

and

$$N_{\Delta n} = \sum_{i=1}^{p} n_i \left(\alpha_i \right)^m .$$

(2.11)

Using the above relations, the following parameters, describing the service-stress spectrum for a structural element, are obtained:

• Maximum-stress-range utilization coefficient for the whole spectrum

$$\alpha_{\max} = \frac{\Delta\sigma_{\max}}{\Delta\sigma_n}, \qquad (2.12)$$

where $\Delta\sigma_{max}$ is the maximum stress range in the spectrum.

- Equivalent-substitute-stress-range coefficient

$$\alpha_e = \frac{\Delta\sigma_e}{\Delta\sigma_n}, \qquad (2.13)$$

which expresses the service utilization of the stress ranges for the whole spectrum with the actual number of cycles N_r. By using the relation (2.10) for $\Delta\sigma_e$ we get the following formula for α_e

$$\alpha_e = \left(\sum_{i=1}^{p} f_i \alpha_i^m\right)^{\frac{1}{m}}. \qquad (2.14)$$

- Single-vehicle-stress-range-utilization correction coefficient (measure of the service single-vehicle harmfulness)

$$\overline{\alpha} = \left(\frac{\Delta\sigma_e}{\Delta\sigma_n}\right) \cdot \left(\frac{N_r}{N_p}\right)^{\frac{1}{m}}, \qquad (2.15)$$

where N_p is the number of vehicles generating the N_r stress cycles. This coefficient was introduced into the Swiss regulations SIA 161 (SIA 1979) and into the European code UIC (CODE UIC 1981). It is a measure of the fatigue harmfulness of a vehicle depending on its profile (number of axles, their configuration and loads), the road traffic parameters, and the kind of bridge element (static scheme, span, number of traffic lanes). If the relation (2.10) is used, this coefficient takes the following form

$$\overline{\alpha} = \left(\sum_{i=1}^{p} f_i \alpha_i^m\right)^{\frac{1}{m}} \cdot \left(\frac{N_r}{N_p}\right)^{\frac{1}{m}}, \qquad (2.16)$$

or if the relation (2.13) is substituted for the first term, one gets

$$\overline{\alpha} = \alpha_e \left(\frac{N_r}{N_p}\right)^{\frac{1}{m}}. \qquad (2.17)$$

- Equivalent substitute number of cycles for the spectrum with the standard-load stress range $\Delta\sigma_n$

$$N_{\Delta n} = N_r \cdot \sum_{i=1}^{p} f_i (\alpha_i)^m \; , \tag{2.18}$$

obtained by rearranging the expressions (2.11) and (2.9).

- Actual single-vehicle number of cycles

$$\overline{N}_r = \frac{N_r}{N_p} \; . \tag{2.19}$$

3. HIGHWAY BRIDGE LOAD MODEL

To carry out the simulation analysis of the service strength of highway bridges one must know the traffic structure and its volume on national highways and bridges.

To the author's knowledge, no study of the service loads acting on the highway bridges in Poland has been made. Besides, that the results of studies and experiments carried out in other countries are not directly applicable to Polish bridges because of the much different load conditions (types of vehicles, traffic density, regulations concerning vehicle technical specifications).

For this reason the author decided to perform own measurements of the road traffic structure and loads, in order to develop a model of the actual service loading of the road bridges in Poland. First, it was necessary to acquire and classify the technical data of vehicles that occur in the actual traffic stream.

A classification of all the basic (distinguishable) types of trucks is presented in table 1.

Fig. 3 shows the traffic structure (including the loading of the particular types of vehicles) on country bridges, urban bridges, and bridges in general.

Fig. 4. shows the histograms of total weights Q_c of trucks for country bridges, urban bridges and road bridges in general, plotted on the basis of the performed measurements. It also shows the vehicle weight Q_c distribution probability density function derived by the author for road bridges in Poland.
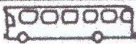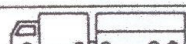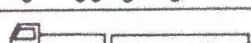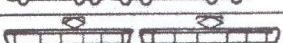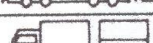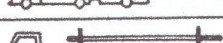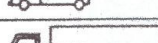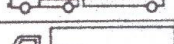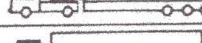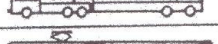
Types of vehicles   Table 1.

No.	Type of vehicle	Denotation	
1		2Sc	
2		2A	2
3		3	
4		2 – 2	
5		2 – 3	
6		3 – 2	2P2
7		3 – 4	
8		4 – 4	
9		2 – 1	
10		2 ○ 1	
11		2S1	
12		2S2	2N1
13		2S3	
14		3S2	
15		4 ○ 2	

Table 1. Types of vehicles

Taking into account the geometry and the construction of trucks, the author divided all the considered types of vehicles into three main groups (tab. 1):

- two-axle single vehicles "2",
- two-axle vehicles with a two-axle trailer "2P2",
- two-axle vehicles with a single-axle "2N1",

for which the appropriate substitute vehicles, constituting the basis for the traffic model and thus representing the whole actual road traffic, were developed.
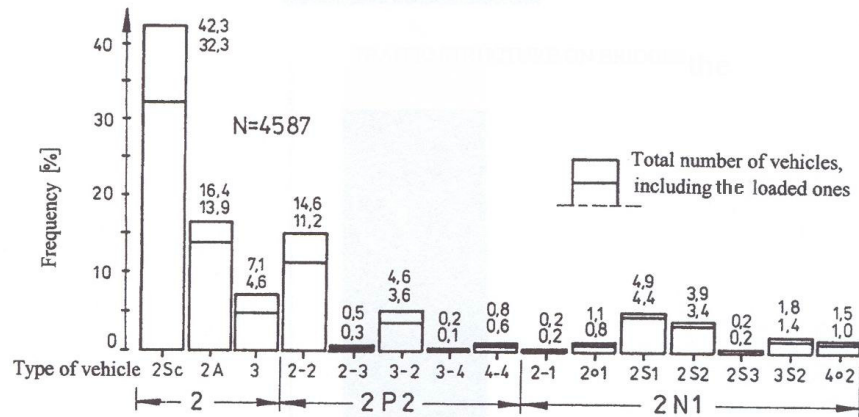
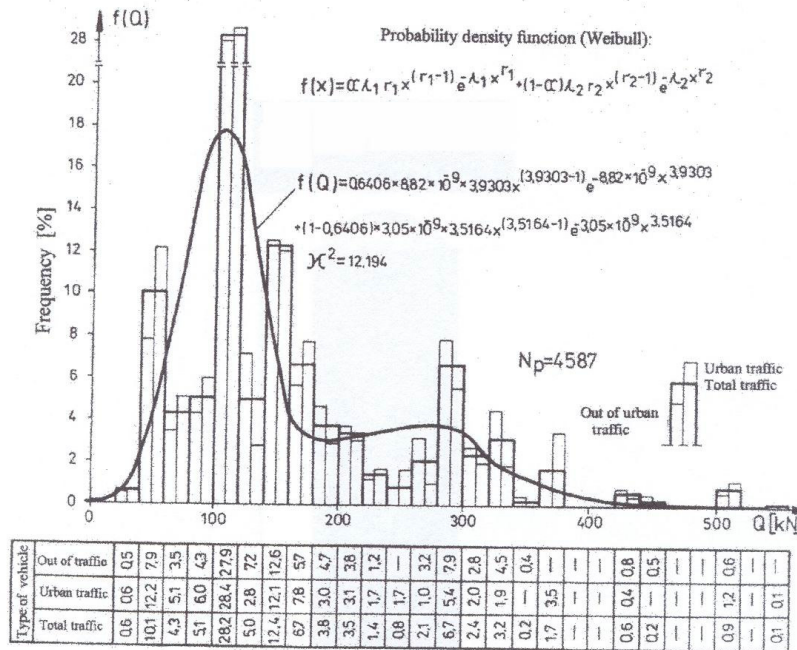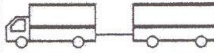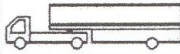Fig. 3. Vehicular traffic structure on highway bridges

Fig. 4. The distribution of total weights of vehicles on highway bridges

The characteristics of the three types of substitute vehicles are given in table 2. The vehicles represent the current national road traffic and so they can be taken as a model of the service loads acting on bridge structures located on the routes of the main national roads in Poland.

Characteristics of substitute vehicles   Table 2.

Types of vehicles	Scheme	a_i	Q_e	q_1	q_2	q_3	q_4	b_1	b_2	b_3
	$q_1 Q$ $q_2 Q$ $q_3 Q$ $q_4 Q$ b_1 b_2 b_3	[%]	[kN]						[m]	
2		65,9	129,6	0,348	0,652	—	—	3,939	—	—
2 P 2		20,6	291,0	0,211	0,377	0,206	0,206	3,973	5,253	3,743
2 N 1		13,5	262,6	0,218	0,356	0,426	—	3,728	5,210	—

Other factors which should be taken into account when describing the vehicular traffic on road bridges (on the country to railway bridges) are: the paths of movement of vehicles within the lane, the transverse distribution of traffic volume and its structure over the traffic lanes (for the determined 24h traffic volumes), the speed of the vehicles and their spacing and the fact that vehicles pass each other on the bridge.

Because of the nature of the road traffic, the above parameters are difficult to define precisely – even on the basis of a large number of surveys. Therefore, the author had to make certain assumptions based on his own researches, described in a more detailed manner in (Wysokowski 1990).

4. DESCRIPTION OF ANALYZED BRIDGE ELEMENTS

Using the TE-MD software, one can determine the stress spectra and the service durability parameters for practically any structural element of any bridge with any static schemes, spans, cross-sections, number of traffic lanes, number of vehicle types, traffic volumes and vehicle speeds. Because of the present paper's limited size, the author cannot analyze all the above cases. Therefore the calculations and the analyses of the stress spectra and the service durability are limited to classical cases, regarding the bridge construction (static schemes, the number of traffic lanes, the number of beams), the types of vehicles, their 24h flows and speeds of travel over the bridge. The particular cases were so selected

as to make possible the assessment of the effect of different parameters on the service durability and to point at the structural elements which are most sensitive to fatigue. Fig.5 shows the bridge-element cross-sections and the static schemes assumed for the calculations.
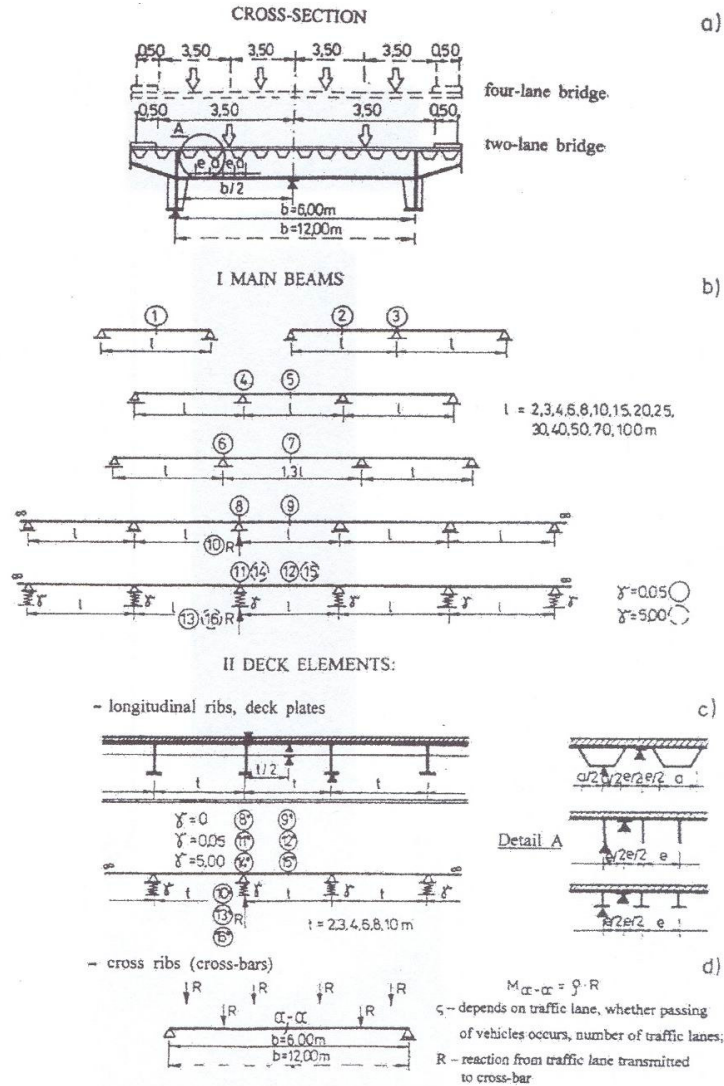

Fig. 5. Structural bridge elements cross-sections and static schemes assumed for calculations

As examples, a two-beam bridge, with both two and four traffic lanes, whose cross-section is shown in fig. 5, was analyzed. The two-beam cross-section represents the most disadvantageous configuration of the main beams, since each vehicle passing over the bridge generates at least one load cycle in their cross-section, regardless of the traffic lane on which it moves.

The calculations were done for the following structural elements:

- main girders,
- cross-beams,
- longitudinal ribs,
- deck plates.

Fig. 5 shows the cross-beams, static scheme assumed for the calculations. This is the most disadvantageous scheme for cross-bars since each vehicle passing over the bridge generates at least one stress cycle in them. Values R, in both two-lane and four-lane bridges, represent the reaction from the particular traffic lanes, transferred onto the ribs, including the deck's flexibility. The cross-bar's central cross-section was adopted for the calculation. The stress ranges are calculated taking into account vehicle passing at different traffic volumes.

5.   RESULTS OF SIMULATION ANALYSIS

5.1. Stress spectra

Since a very large number of calculation results were obtained, the author had to select only the most significant ones and to present them in the most concise form to fit them into the present paper.

Figs 6a,b,c and 7 show the sample computational stress spectra and their distribution functions (10, 50, 90 and 100%) for the selected main-girder systems of the two-lane bridge. For comparison, fig. 8 shows the sample stress-range spectra for the simple-supported main girders of the four-lane bridge.

Computational stress-range spectra for the deck elements, at different flexibility coefficients γ and different cross-beam spacing t, are presented in fig. 9 (for longitudinal ribs) and fig. 10 (for cross-beams).

5.2. Calculated service strength parameters

Besides the stress spectra, the computer simulation analysis yielded the service strength parameters for the consecutive numbers of main-girder and deck-element systems. The parameters for the particular systems depend on the span length, the 24h traffic volume and the driving speed of vehicles.
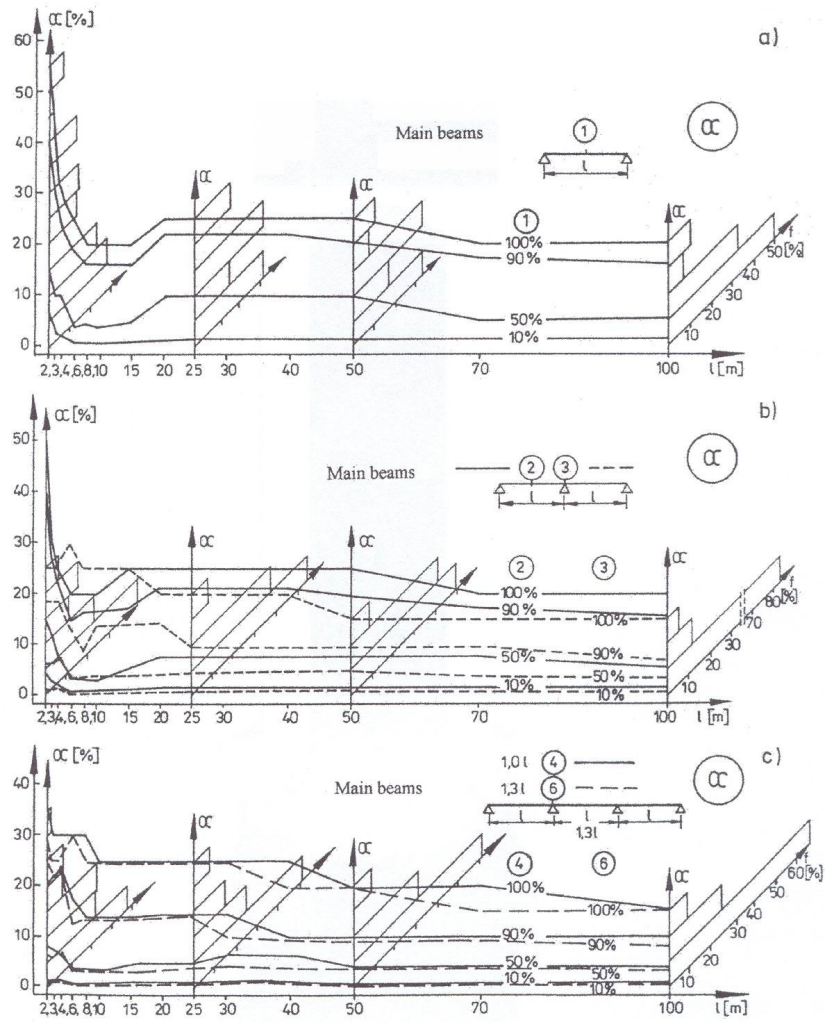
Fig. 6. Computational stress-range spectra for main girders of two-lane bridge
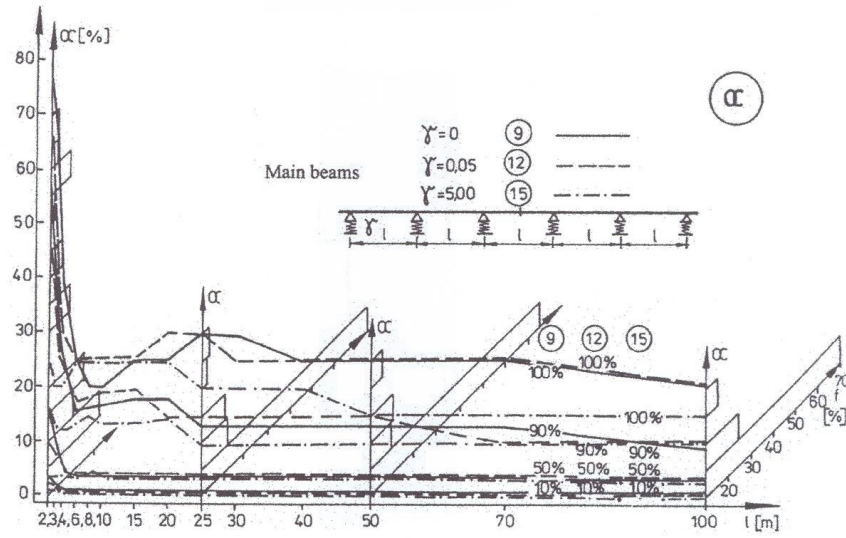
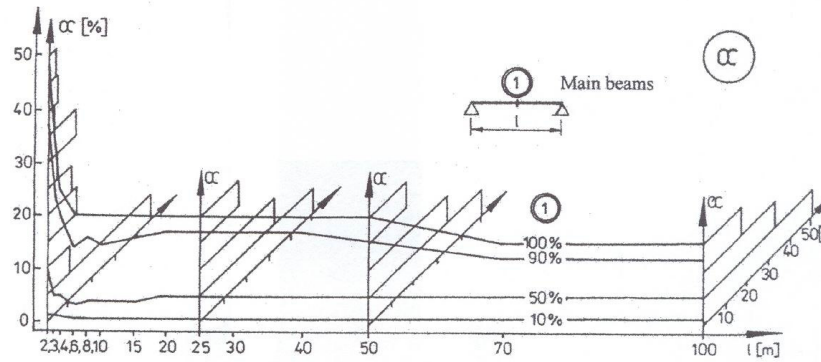Fig. 7. Computational stress-range spectra for main girders of two-lane bridge

Fig. 8. Computational stress-range spectra for main girders of four-lane bridge
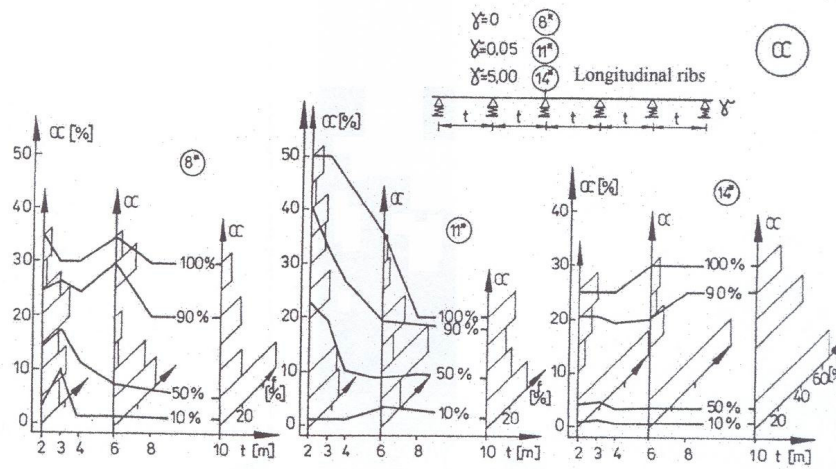
Fig. 9. Computational stress-range spectra for longitudinal ribs for different flexibility coefficients γ
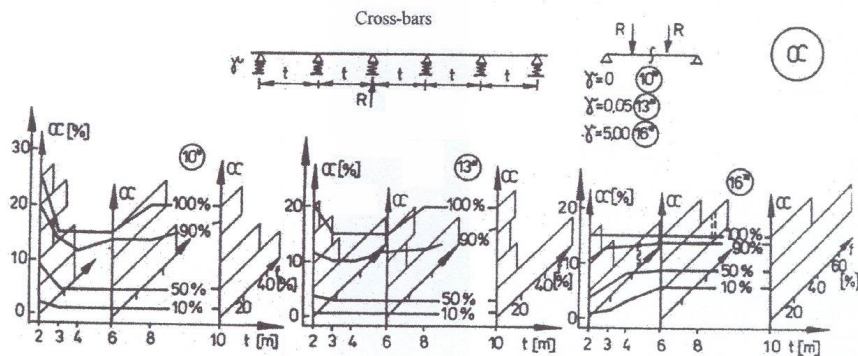
Fig. 10. Computational stress-range spectra for cross-beams at different flexibility coefficients γ

Figs 11a and b, 12a and b and 13a and b show graphs of the equivalent substitute stress-range coefficient α_e and the maximum stress-range utilization coefficient α_{max}, for the particular main-girder systems of the two-lane bridge, depending on span length l at 24h traffic volume $N_p^d = 1$ and 7000 vehicles and speed $v = 13.9$ m/s.

Fig. 11. Graphs of equivalent substitute stress-range coefficient α_e and maximum stress-range utilization coefficient α_{max} for main girders of two-lane bridge

Fig. 12. Graphs of equivalent substitute stress-range coefficient α_e and maximum stress-range utilization coefficient α_{max} for main girders of two-lane bridge

Fig. 13. Graphs of equivalent substitute stress-range coefficient α_e and maximum stress-range utilization coefficient α_{max} for main girders of two-lane bridge

For comparison, fig. 14 shows the graphs of coefficients α_e and α_{max} for the simply supported main girders of the four-lane bridge at 24h traffic volume $N_p^d = 1$ and 14000 vehicles and speed $v = 13.9$ m/s.
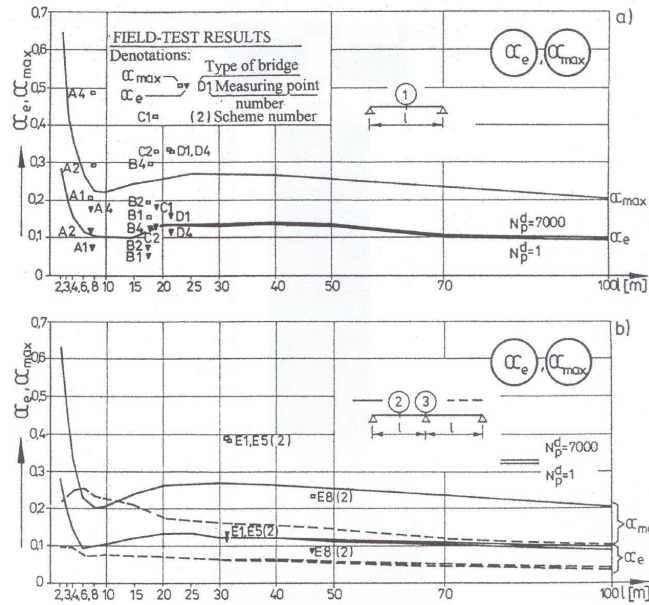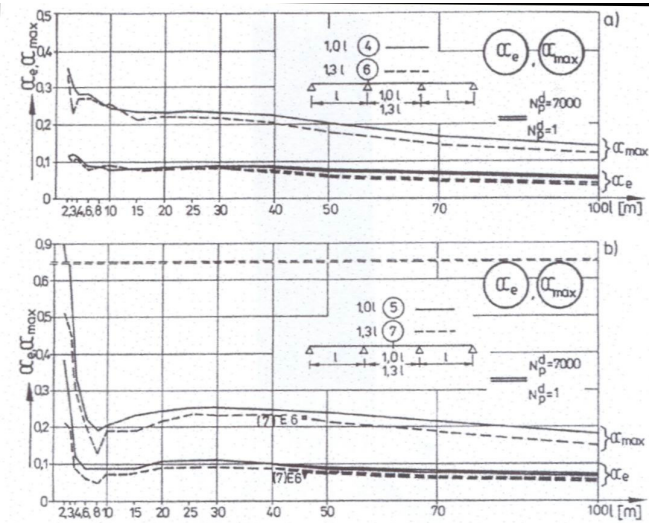

Fig. 14. Graphs of equivalent substitute stress-range coefficient α_e and maximum stress-range utilization coefficient α_{max} for main girders of four -lane bridge
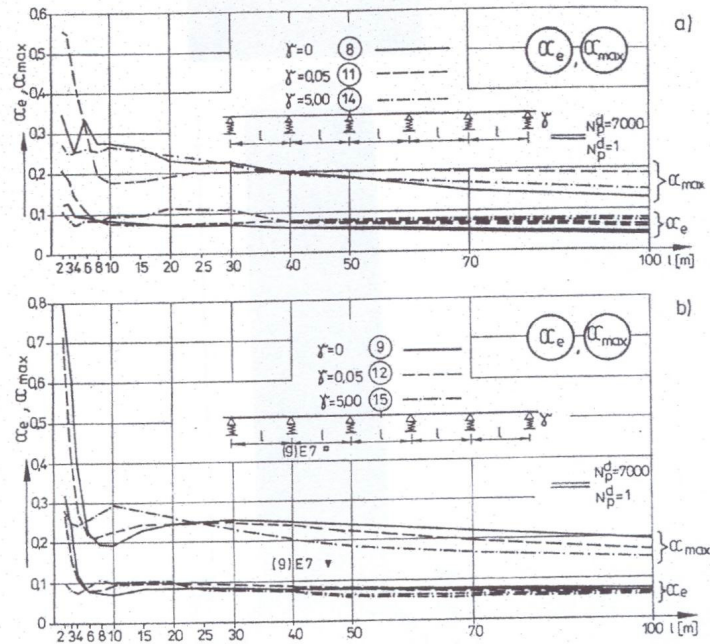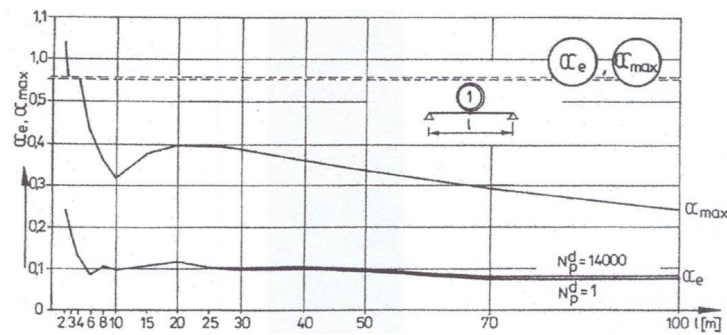
Graphs of coefficients α_e and α_{max} for the deck elements are shown in figs 15a and b (for longitudinal ribs and deck plates) and fig. 16 (for cross-beams).

Fig. 15. Graphs of equivalent substitute stress-range coefficient α_e and maximum stress-range utilization coefficient α_{max} for longitudinal ribs (a, b) and deck plates (b)
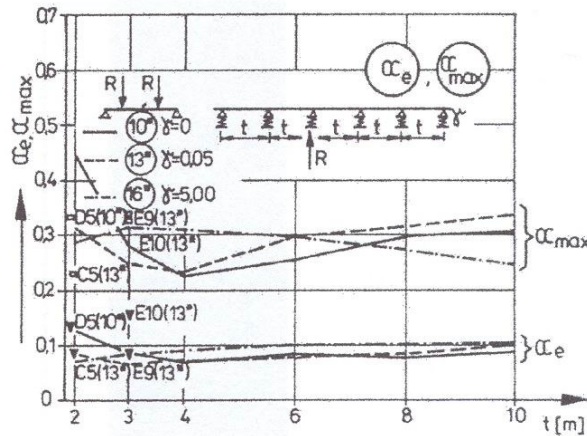
Fig. 16. Graphs of equivalent substitute stress-range coefficient α_e and maximum stress-range utilization coefficient α_{max} for cross-beams

Figs 17a, b, c, d and 18a, b show traces of the single-vehicle-stress-range-utilization correction coefficient $\overline{\alpha}$ (a measure of single-vehicle service harmfulness) for the particular numbers of the main-beam systems of the two-lane bridge versus span length l for 24h traffic volume $N_p^d = 1$ and 7000 vehicles and speed $v = 13.9$ m/s.

Fig. 17. Graphs of single-vehicle stress-range utilization correction coefficient $\overline{\alpha}$ for main girders of two-lane bridge

Fig. 18. Graphs of single-vehicle stress-range utilization correction coefficient $\overline{\alpha}$ for
main girders of two-lane bridge

Fig. 19 shows the trace of the coefficient $\overline{\alpha}$ for the simple-supported
main girders of the four-lane bridge at 24h traffic volume $N_p^d = 1$ and 14000
vehicles and speed $v = 13.9$ m/s.
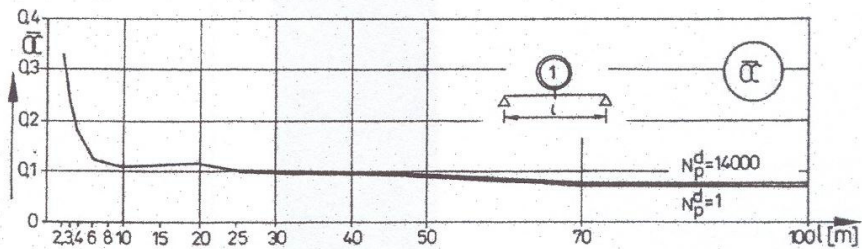
Fig. 19. Graphs of single-vehicle stress-range utilization correction coefficient $\overline{\alpha}$ for
main girders of four-lane bridge

Graphs of the correction coefficient $\bar{\alpha}$ for a deck element are shown in fig. 20a,b (for longitudinal ribs and deck plates) and fig. 21 (for cross-beams).
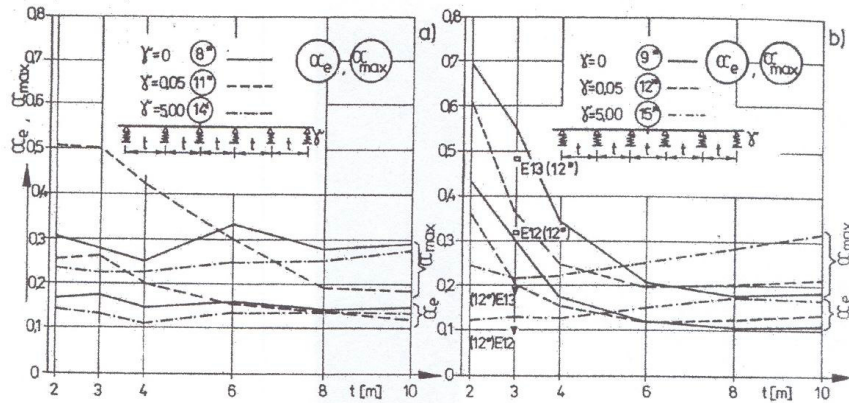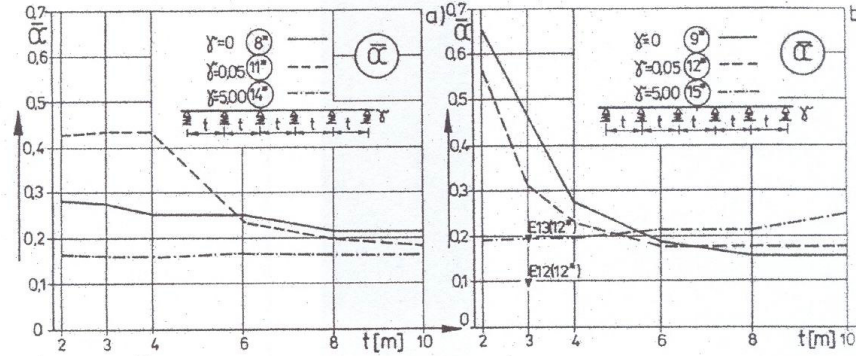
Fig. 20. Graphs of single-vehicle stress-range utilization correction coefficient $\bar{\alpha}$ for longitudinal ribs (a, b) and deck plates (b) at different flexibility coefficients γ
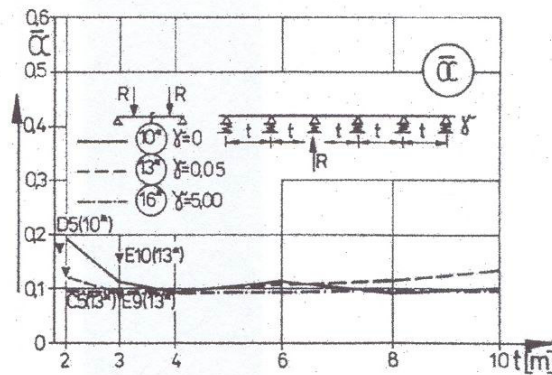
Fig. 21. Graphs of single-vehicle stress-range utilization correction coefficient $\bar{\alpha}$ for cross-beams at different flexibility coefficients γ

Figs 22a,b, 23a,b and 24a,b show graphs of actual numbers of single-vehicle cycles $\bar{N}_r$ for the particular main-beam systems of the two-lane bridge versus span length l for 24h traffic volume $N_p^d = 1$ and 7000 vehicles and speed $v = 13.9$ m/s.

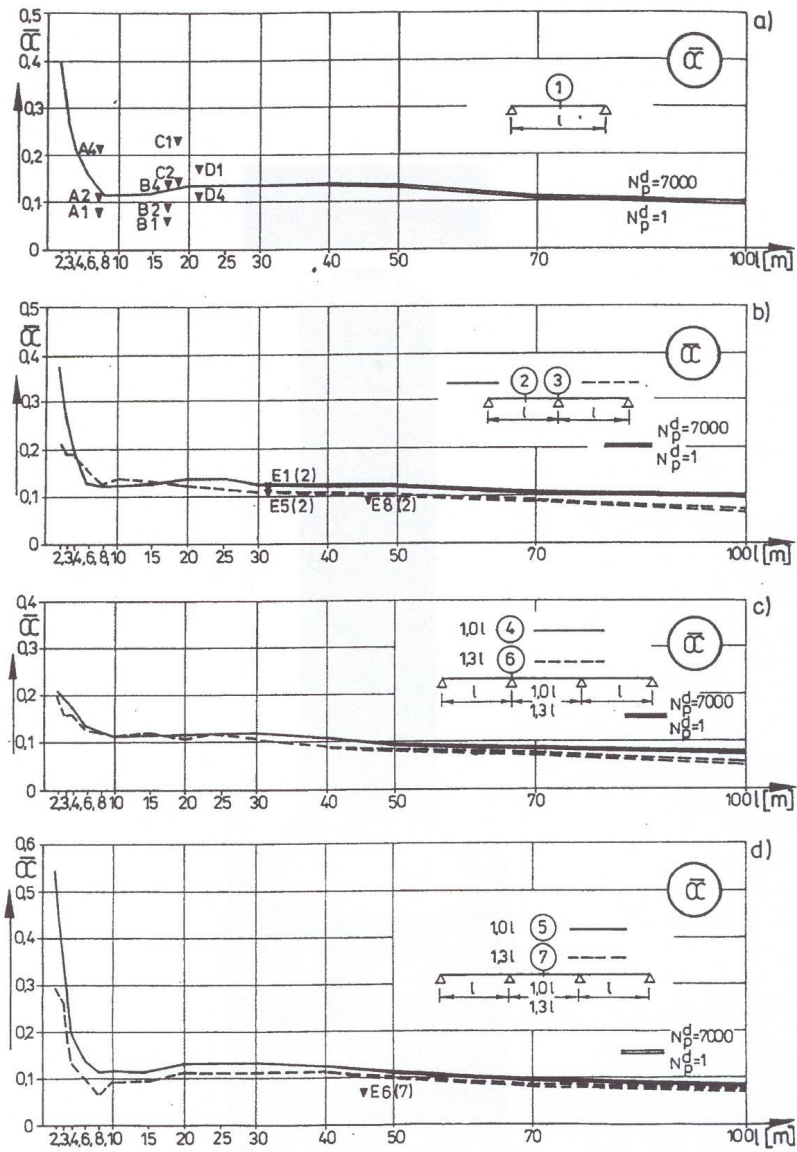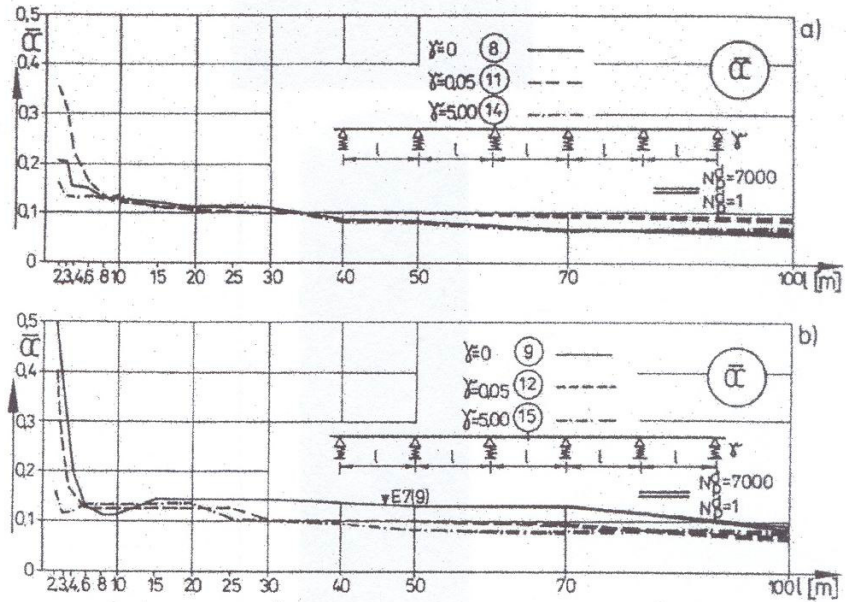Fig. 25 shows graphs of values $\bar{N}_r$ for the simply supported main girders of the four-lane bridge at 24h traffic volume $N_p^d = 1$ and 14000 vehicles and speed $v = 13.9$ m/s.
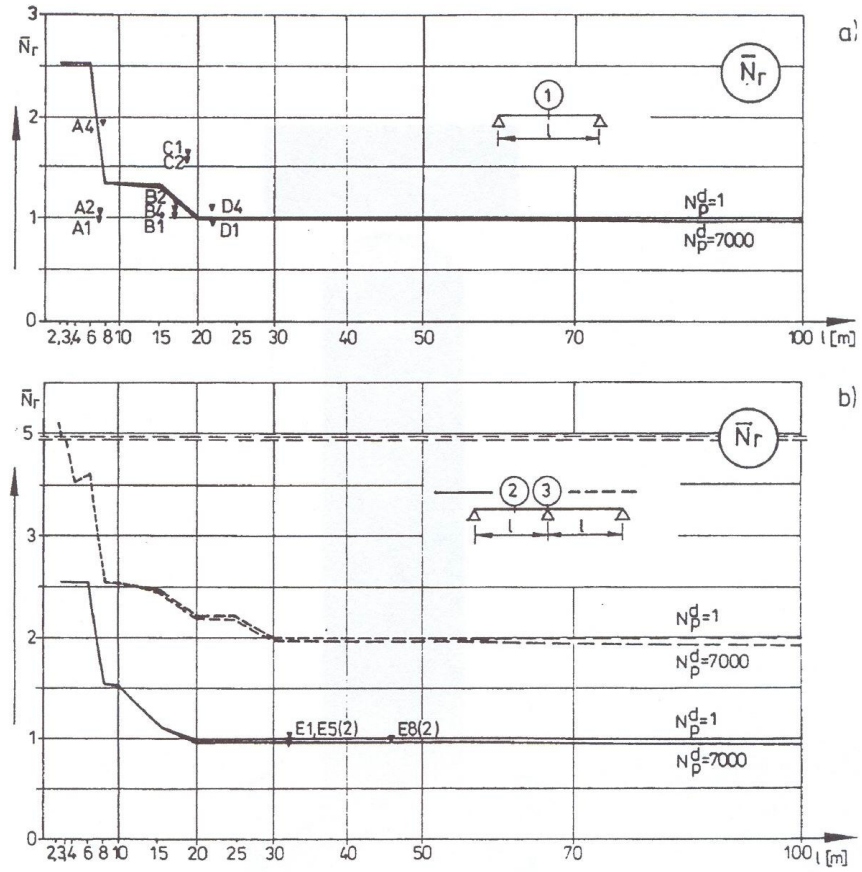
Fig. 22. Graphs of actual numbers of cycles generated by one vehicle $\overline{N}_r$ for main girders of two-lane bridge
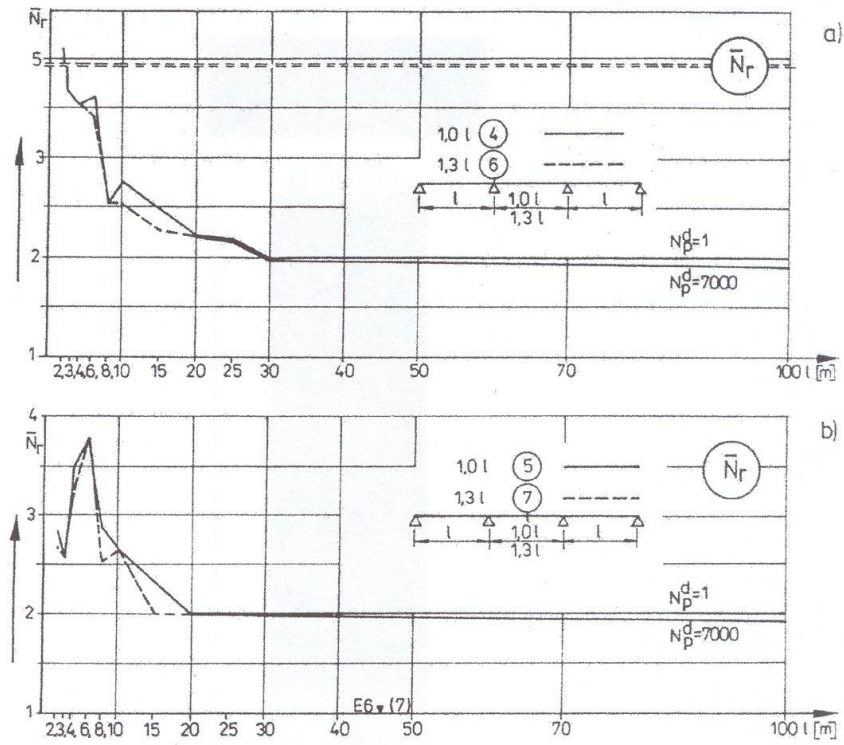
Fig. 23. Graphs of actual numbers of cycles generated by one vehicle $\overline{N}_r$
for main girders of two-lane bridge
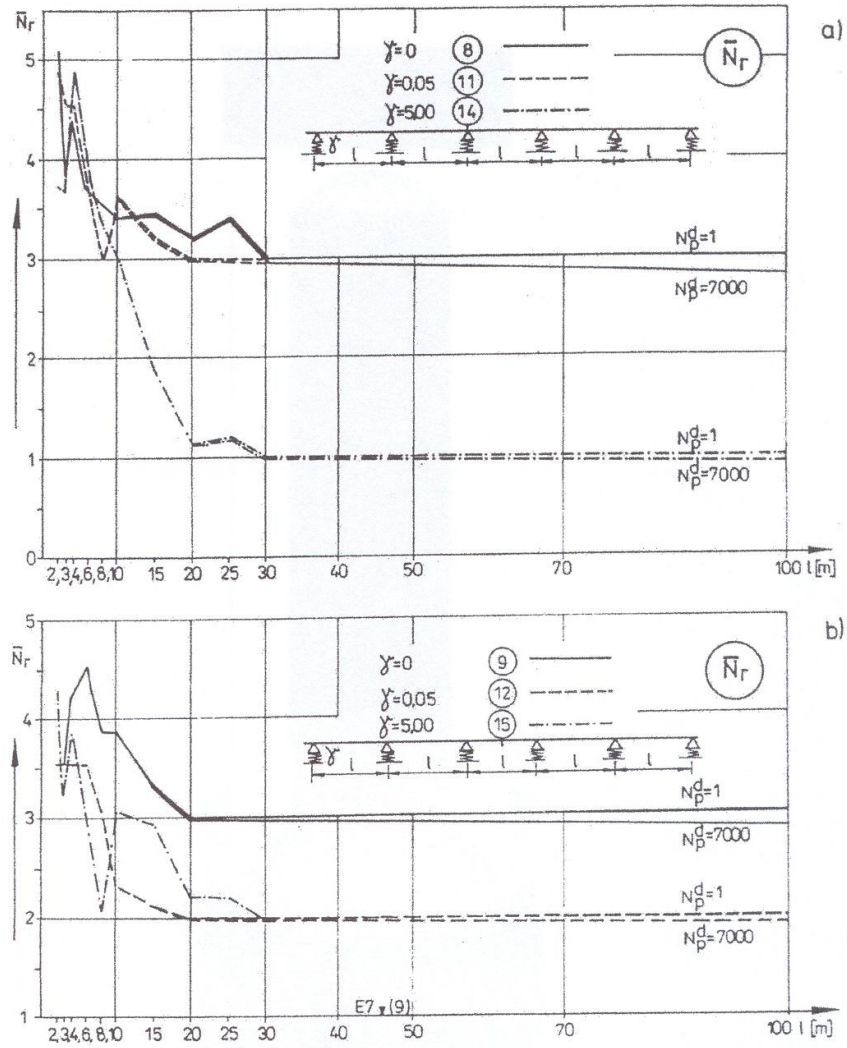
Fig. 24. Graphs of actual numbers of cycles generated by one vehicle $\overline{N}_r$ for main girders of two-lane bridge

Graphs of the parameter $\overline{N}_r$ for a deck element depending on longitudinal spacing of cross-beams (*t*) at different flexibility coefficients γ, are shown in fig. 26a,b (for longitudinal ribs and deck plates) and fig. 27 (for cross-beams).

Fig. 25. Graphs of actual numbers of cycles generated by one vehicle $\overline{N}_r$
for main girders of four-lane bridge

Fig. 26. Graphs of actual numbers of cycles generated by one vehicle $\overline{N}_r$
for longitudinal ribs (a, b) and deck plates (b)

Fig. 27. Graphs of actual numbers

6. ANALYSIS OF SERVICE STRENGTH RESULTS

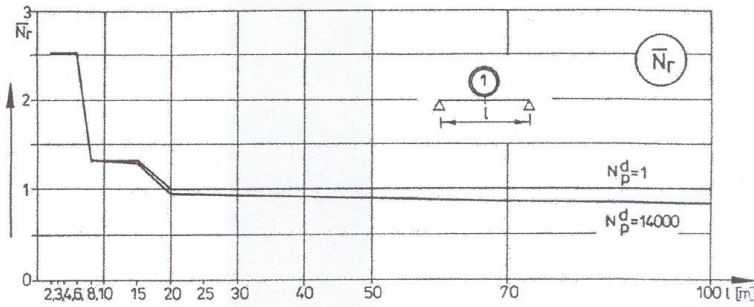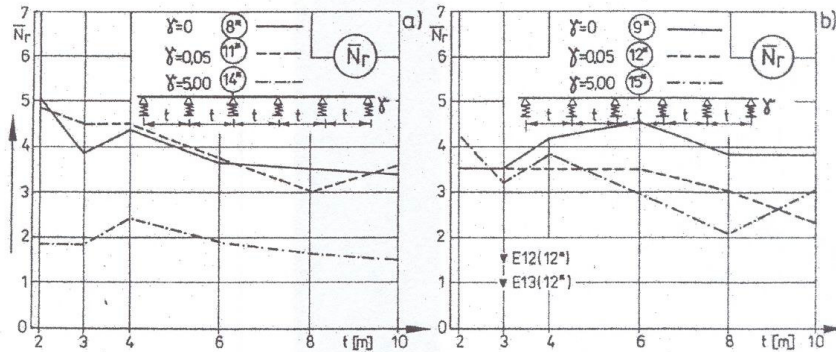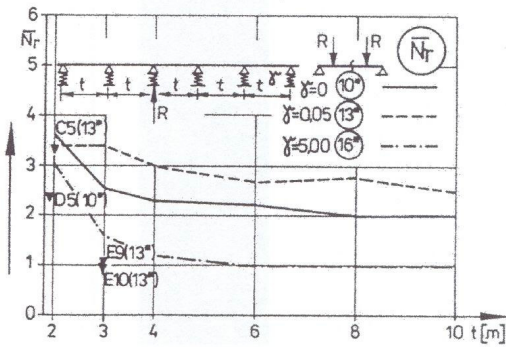Examining the collected stress-range spectra for the simply supported main girders of the two-lane bridge (fig. 6), one can notice that their peak ranges α_i occur at short span lengths (1 = 2-6 m) and then at 20-50 m. Their lowest values and the highest frequency of occurrence of narrow-stress-range cycles are observed at span lengths of 6-15 m. In addition, the trace of the 50% distribution function indicates that over 50% of the service cycles have stress ranges narrower than 10% of the standard-load stress range $\Delta\sigma_n$.

A comparison of the stress-range spectra for the mid-span cross-section with those for the support cross-section of the continuous two-span girder of the two-lane bridge (fig. 6) shows that for the span lengths shorter than 4 m and span lengths longer than 15 m the stress-range values for the mid-span cross-section are higher than for the support cross-section whereas for span lengths of 4-15 m the opposite is true.

A similar comparative analysis for the continuous three-span girder support cross-section for different lengths of the central span (1.01 and 1.31) (fig. 6) shows that higher stress-range values were obtained for the girder having all spans of equal length. For the two three-span schemes over 50% of the total number of service cycles has a stress range narrower than 5% of the stress range $\Delta\sigma_n$ (generated by standard load).

The highest stress-range values in a spectrum were obtained for the span cross-section of a girder with an infinite number of spans (fig.7) on rigid supports, with the span length of 2.0 m (α =75%).

For a beam with an infinite number of spans on flexible supports the obtained stress-range values are on the whole lower than for the beam on rigid supports.

A comparison of the stress-range spectrum for the single-span simply supported main girder of the four-lane bridge (fig. 8) with the corresponding spectra for the two-lane bridge (fig. 6) shows that the stress-range values in the former case are lower than in the latter case. In addition, the frequency of the occurrence of lower stress-range values, in the case of the main girder of the four-lane bridge, is higher than the corresponding frequency for the main girder of the two-lane bridge, as indicated by, among other things, the traces of relevant distribution functions (10% and 50%).

The highest stress-range-spectrum values are approximately constant, irrespective of the longitudinal spacing t and the flexibility γ of the cross-bars, for both the longitudinal rib support cross-section (fig. 9) and the deck cross-beams (fig. 10). Only for the longitudinal rib support cross-section at the flexibility γ = 0.05 (most common in the case of orthotropic bridge plates) for the narrow

spacing of cross-beams: t = 2.0-6.0 m, the stress-range values are higher (40-50%).

The analysis of graphs of the equivalent substitute stress range coefficient α_e and maximum stress range utilization coefficient α_{max} for the particular bridge elements, presented in figs 11-16, shows that:

- The values of coefficients α_{max} and α_e depend on span length l – for the main girder or spacing of the cross-beams t – for the deck elements.
- The α_{max} graphs run roughly parallel to the α_e graphs in the case of both the main beams and the deck elements.
- The highest value of the service stress range utilization coefficient α_e for the main beams was recorded for the mid-span section of the three-span girder with equal span lengths (system no. 5): α_e = 0.379 at l = 2.0 m.
- Service stress range utilization α_e for the cross-bars is on the whole independent of their flexibility and their spacing in the deck t.
- The highest service stress range utilization α_e occurs in the case of the deck plates and the longitudinal rib mid-span cross-section when the cross-bars are rigid (system no. 9) and spaced longitudinally at t = 2.0 m – α_e = 0.433. For the above scheme and parameters, the highest maximum stress-range value – α_{max} = 0.692 – was recorded for the deck.

The graphs of the single-vehicle-stress-range-utilization correction coefficient $\overline{\alpha}$, shown in figs 17-21 for the particular road bridge elements, have a close similarity to the respective graphs of the equivalent substitute stress range α_e. The similarity follows from, among other things, the form of formula (2.17). In the case of simply supported girder of shorter spans (particularly with continuous static schemes) and deck elements, the actual number of cycles is, as a rule, much larger than the number of vehicles that pass over the bridge. Thus, in such cases, the values $\overline{\alpha}$ are appropriately higher than the values α_e.

The analysis of the graphs of the actual single-vehicle number of cycles $\overline{N}_r$ presented in figures 22-27 for the particular structural elements shows that:

- Number of cycles $\overline{N}_r$ depends on the cross-section and the static scheme, as well as on the span length l - in case of the main girders, and on the longitudinal spacing of cross-beams t - for the deck elements.
- In case of the main girders, the graphs of the actual number of cycles per vehicle $\overline{N}_r$ goes down to $\overline{N}_r$ = 1.0; 2.0 or 3.0, as the span length increases to 20.0 m (for mid-span cross-sections) and 30.0 m (for support cross-sections), depending on the system. As the span length l increases further, the graphs' course runs horizontally (constant number of cycles $\overline{N}_r$). This shape of the graphs and their local inflexions are determined by the axle base

and the system relative to the length of the influence-line branches depending on a static scheme and the span length.

- Generally, the average number of stress-range cycles per vehicle is larger for support cross-sections than for the mid-span cross-sections.
- For the three-span continuous girder with spans of equal length (for both the support cross-section and the mid-span cross-section), the actual single-vehicle number of stress-range cycles $\overline{N}_r$ is slightly larger than for the scheme in which the central span is longer than the side ones.
- A noticeable effect of vehicles passing each other on the bridge on the number of stress-range cycles per vehicle $\overline{N}_r$ is recorded in the case of the main girders for span lengths over 15.0-20.0 m, and as the span length and 24h traffic volume N_p^d increase, the actual number of cycles per vehicle $\overline{N}_r$ decreases (due to the simultaneous generation of stress-range cycles by the vehicles passing each other).
- Taking into account the most common main girder span lengths and the typical longitudinal spacing of cross-bars in the orthotropic plate typical for road bridge structures, it can be stated that larger numbers of single-vehicle stress-range cycles $\overline{N}_r$ occur for the deck elements than for the main girders.

7. COMPARATIVE ANALYSIS OF SIMULATION CALCULATION RESULTS AND IN SITU TEST RESULTS

To compare the field test results with the simulation results, the author calculated, using the formulas given in chapter 2, the service strength and durability parameters for the elements of tested bridge structures. The calculations were based on the stress-range histograms obtained from the tests carried out on actual bridge structures. The field test results for the elements of the steel highway bridges were plotted on the graphs of the corresponding parameters, obtained from computer simulations.

The field-test values of the equivalent substitute stress-range coefficient α_e and the maximum stress-range utilization coefficient α_{max} for the elements were plotted in figs 11-13, 15 and 16.

The field-test values of the single-vehicle stress-range utilization correction coefficient $\overline{\alpha}$ for the elements were plotted on the graphs shown in figs 17, 18, 20 and 21.

The field-test values of the actual single-vehicle number of cycles $\overline{N}_r$ for the elements were plotted on the graphs in figs 22-24, 26 and 27.

To sum up, the field-test values of the service strength for the considered elements have proved the assumptions made for the theoretical calculations and the obtained agreement between the test results and the calculation results confirms the computer simulation analyses of the service durability.

8. CONCLUSIONS

On the basis of the analysis made in this paper the following general conclusions can be drawn:

1. The simulation computer software developed by the author makes it possible to enter the data necessary for calculations and to obtain results in a concise form, on the basis of which a quick assessment of the service strength and durability can be made for any type of bridges with different static schemes, span lengths, cross-sections, number of traffic lanes, for any number of types of vehicles and their characteristics for different traffic volumes and vehicle travelling speeds.
2. The substitute-vehicle stress-range values yielded by the computer simulation, similarly as those obtained from field tests on actual bridges, are much lower (by 15-75% depending on the kind of element and its span) than the calculated standard-moving-load stress-range values.
3. The field-test values of service strength obtained for the considered elements have proved the assumptions made for the theoretical calculations and thus they have validated service durability analyses made by computer simulation.
4. All the structural elements of the steel spans of highway bridges are sensitive to fatigue and this hazard depends on such factors as: the kind of element, the static scheme, the flexibility of the supports, the length of the spans, the 24h traffic volume, the travelling speed of vehicles, the kind of steel and the type of notch.
5. Generally, elements with continuous static schemes are more sensitive to fatigue than the simply supported single-span elements.
6. In the case of the main girders it has been found that:
    * The fatigue hazard is directly linked to the length of the spans and it is the greatest for span lengths below 8.0 m and then for span lengths in the range of 20.0-40.0 m. For span lengths 8.0-15.0 m and over 40.0 m the fatigue hazard is relatively small.
    * In case of continuous three-span girders, as the length of the central span increases relative to the side spans, the fatigue hazard to of girders eases.

- The main girders of bridges with two traffic lanes are more exposed to fatigue hazard than the ones in bridges with a larger number of traffic lanes.
- The fatigue hazard for the mid-span cross-sections is greater than to support section, regardless of the number of spans.
- As the flexibility of the main girders increases, their fatigue hazard decreases.

7. Generally, the deck elements are more sensitive to fatigue than the main girders. Furthermore, it has been established that:
   - As the longitudinal spacing of the cross-bars in the grate decreases, so does the fatigue hazard for the longitudinal ribs.
   - As the flexibility of the cross-beams increases, the fatigue hazard for the deck elements (deck plates, longitudinal ribs and cross-bars) decreases.
   - The most serious fatigue hazard occurs in the longitudinal ribs. Under the current maximum 24h traffic volume N_p^d = 4000, regardless of the kind of steel and the type of notch, one should be concerned about the fatigue in the longitudinal ribs for any spacing of cross-bars in the deck and any flexibilities of the cross-bars.

The simulation EMC software developed by the author and the presented approach to the assessment of the service strength and durability of highway bridges can be applied, without any limitations, to similar analyses of the span elements of one-track and two-track railway bridges with any static schemes.

REFERENCES

1. Baus R., Bruls A. (1981). Etude du comportement des ponts en acier sous l'action du trafic routier. Détermination des actions pour le calcul statique et le calcul à la fatigue. Centre de recherches scientifiques et techniques de l'industrie des fabrications métalliques, CRIF, Bruxelles.
2. B. S. (1980). 5400: Steel, Concrete and Composite Bridges, Part 10: Code of Practice for Fatigue. British Standards Institution, London.
3. Carpena A. (1982). Fatigue Design Concept of the ECCS. *IABSE Colloquium "Fatigue of Steel and Concrete Structures"*, Laussanne, Switzerland, IABSE Proceedings, vol. 37, pp.7 – 14.
4. Code UIC 778 – 1R. (1981). Recommandations relatives aux facteurs de fatigue a considerer lors du dimensionnement des ponts métalliques de chemin de fer. UIC, Paris.
5. Czudek H., Pietraszek T. (1980). *Trwałość stalowych konstrukcji mostowych przy obciążeniach zmiennych*. WKiŁ, Warszawa.

6. Hirt M. A. (1977). Neue Erkenntnisse auf dem Gebiet der Ermüdung und deren Berücksichtigung bei der Bemessung von Eisenbahnbrücken. *Bauingenieur* J. 52, H. 7, pp. 255 – 262.

7. Hirt M. A. (1983). Réserve de durée de vie des ponts. *Construction Métallique*, no.1, pp. 3 – 13.

8. IIW (1981). International Institute of Welding, Design Recommendations for Cyclic Loaded Welded Steel Structures. Document JWG–XII–XV-53-81, Paris, France.

9. SIA 161 (1979). Norme , Constructions Métalliques. Societe Suisse des Ingénieurs et des architectes /SIA/, Zurich, Switzerland.

10. Stier W., Steinhardt O., Valtinat G., Kosteas D. (1982). Residual Fatigue Life of Railway Bridges. *IABSE Colloquium "Fatigue of Steel and Concrete Structures"* Lausanne, Switzerland, IABSE Proceedings, vol. 37, pp. 823 – 831.

11. Wysokowski A. (1990). Wpływ losowości ruchu drogowego na wytrzymałość eksploatacyjną mostów. *Prace Instytutu Badawczego Dróg i Mostów*, no 2, pp. 150-170.

12. Wysokowski A. (1989). Durability Aspects in the Design of Steel Highway Bridges. *IABSE Symposium "Durability of Structures"* Lisbon, Portugal. IABSE Proceedings, vol. 57/2, pp. 475-480.

13. Wysokowski A. (1985). "Operational Strength of Steel Spans of Road Bridges",(in Polish), Doctoral Thesis,, *Raporty Instytutu Inżynierii Lądowej Politechniki Wrocławskiej*, PRE nr 37.

14. Wysokowski A., Łęgosz A. (1995). Monitoring of Bridge Conditions for Durability Evaluation in Poland. *IABSE Symposium "Extending the Lifespan of* Structures" San Francisco 1995.

15. Wysokowski A. (1985). Estimation of the Operational Durability of Steel Highway Bridges by the Simulation Method. *Proceedings of ICOSSAR '85, the 4th International Conference on Structural Society and Reliability*. The International Conference Center Kobe, Japan May 27 – 29.

16. Wysokowski A. (1990). Overview of Some Research Projects on Durability of Bridges. *Proceedings Bridge Engineering Research in Progress*. National Science Foundation and Civil Engineering Department University of Nevada, Reno.

NOTATION

f_i – relative frequency of number of cycles n_i

p – number of stress-range levels in the considered no stationary spectrum

$p(x)$ – force values along the length of an influence line,

q_k – transverse load-distribution coefficient for lane k,

t – different cross-bars spacing

$y(x)$ – ordinates of the influence line of a static quantity (moment or a reaction) for a considered cross-section

N_r – actual number of cycles

$N_{\Delta n}$ – equivalent number of cycles

N_p – number of vehicles generating N_r stress cycles

Q_c – total weights of trucks for country bridges

a – static strength constant,

α_e – equivalent substitute stress-range coefficient

α_{max} – maximum stress-range utilization coefficient

$\overline{\alpha}$ – correction coefficient for a deck element

γ – different flexibility coefficients

$\Delta\sigma_e$ – equivalent stress range

$\Delta\sigma_i$ – expression for the next value of stress

$\Delta\sigma_n$ – standard-load stress range

σ_{min} – absolute value of minimum stress

$\Delta\sigma_{max}$ – maximum stress range in the spectrum

$\varphi_{\Delta actual}$ – dynamic actual-load stress-range coefficient

$\varphi_{\Delta stand.}$ – standard-load stress range dynamic coefficient